

Research



Cite this article: Majkut JD, Carter BR, Frölicher TL, Dufour CO, Rodgers KB, Sarmiento JL. 2014 An observing system simulation for Southern Ocean carbon dioxide uptake. *Phil. Trans. R. Soc. A* **372**: 20130046. <http://dx.doi.org/10.1098/rsta.2013.0046>

One contribution of 12 to a Theo Murphy Meeting Issue ‘New models and observations of the Southern Ocean, its role in global climate and the carbon cycle’.

Subject Areas:

biogeochemistry, oceanography

Keywords:

carbon, Southern Ocean, observational system simulation experiment

Author for correspondence:

Joseph D. Majkut
e-mail: jmajkut@princeton.edu

An observing system simulation for Southern Ocean carbon dioxide uptake

Joseph D. Majkut¹, Brendan R. Carter¹,
Thomas L. Frölicher², Carolina O. Dufour¹,
Keith B. Rodgers¹ and Jorge L. Sarmiento¹

¹Atmospheric and Oceanic Sciences Program, Department of Geosciences, Princeton University, Princeton, NJ 08544, USA

²Environmental Physics, Institute of Biogeochemistry and Pollutant Dynamics, ETH Zürich, 8092 Zürich, Switzerland

The Southern Ocean is critically important to the oceanic uptake of anthropogenic CO₂. Up to half of the excess CO₂ currently in the ocean entered through the Southern Ocean. That uptake helps to maintain the global carbon balance and buffers transient climate change from fossil fuel emissions. However, the future evolution of the uptake is uncertain, because our understanding of the dynamics that govern the Southern Ocean CO₂ uptake is incomplete. Sparse observations and incomplete model formulations limit our ability to constrain the monthly and annual uptake, interannual variability and long-term trends. Float-based sampling of ocean biogeochemistry provides an opportunity for transforming our understanding of the Southern Ocean CO₂ flux. In this work, we review current estimates of the CO₂ uptake in the Southern Ocean and projections of its response to climate change. We then show, via an observational system simulation experiment, that float-based sampling provides a significant opportunity for measuring the mean fluxes and monitoring the mean uptake over decadal scales.

1. Introduction

The Southern Ocean plays a central role in shaping the global ocean's circulation and biogeochemical cycling. At latitudes near the Drake Passage, the Southern Ocean lacks meridional boundaries, which allows for two closely related phenomena. First, the strong, eastward-flowing Antarctic Circumpolar Current (ACC) connects

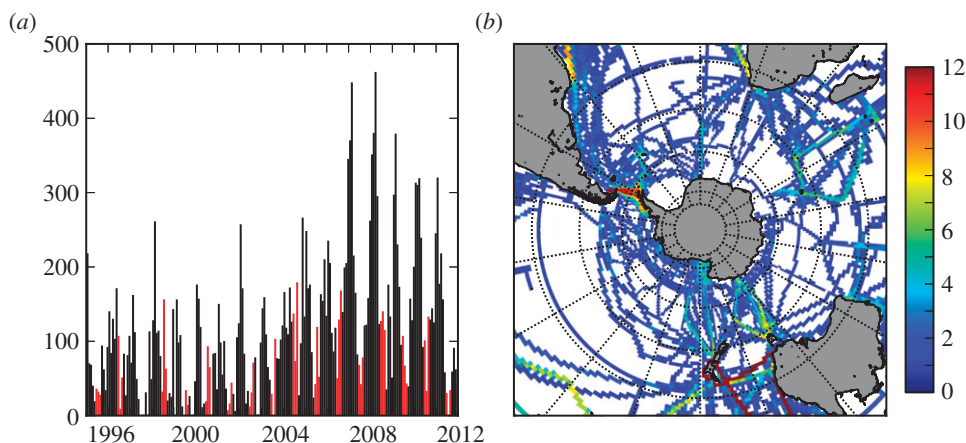


Figure 1. The number of surface measurements of $p\text{CO}_2$ in gridded SOCAT v2, between 1995 and 2012. (a) Total monthly observations, south of 30°S , with winter months (June–August) in red. (b) Calendar months occupied, where 12 indicates full occupation of the seasonal cycle and white indicates no available measurements.

the Atlantic, Pacific and Indian Ocean basins, allowing for mixing of water masses between the basins. Second, the westerly winds drive significant upwelling of old and nutrient-rich waters from the deep ocean, which are almost free of anthropogenic carbon, where they can interact with the atmosphere. Because of these properties, the Southern Ocean closes the overturning circulation of the global ocean [1], maintains the nutrient balance of the low-latitude oceans [2] and sequesters anthropogenic CO_2 and excess heat from the atmosphere [3].

The processes that control the Southern Ocean's circulation and biogeochemistry, and thus a big part of the global ocean's, remain unresolved. Direct measurements provide limited information through time and space, because the sampling that is available is sparse and biased towards summer months. This is particularly the case for biogeochemical observations [4,5]. For example, the surface $p\text{CO}_2$ measurements that provide critical constraints on the sea–air CO_2 flux leave many months and areas of the Southern Ocean unsampled (cf. figure 1). In contrast to measurements, general circulation models (GCMs) provide complete information on a model grid. However, current GCMs rely on parametrizations to simulate subgrid-scale processes, such as mesoscale eddy processes. Mesoscale eddies govern much of the Southern Ocean dynamics, and the reliance on parametrizations of their effects decreases confidence in model results and projections [6]. Likewise, biological models are incomplete representations of the ecology and production within the Southern Ocean. Together, the sparsity of the data and the incomplete nature of model simulations create significant opportunity for continued learning about the Southern Ocean.

The focus of this work is the Southern Ocean CO_2 uptake. Fluxes of anthropogenic CO_2 across the surface of the Southern Ocean are thought to account for up to 50% of the total oceanic uptake [4]; however, storage of anthropogenic CO_2 is small in the Southern Ocean compared with the *in situ* fluxes. A large proportion of the total uptake of CO_2 accumulates in Subantarctic mode water and Antarctic intermediate water [7] and flows into other ocean basins [8]. The oceanic uptake itself amounts to 25% of annual CO_2 emissions from burning fossil fuels and land-use change [9]. The primacy of the Southern Ocean flux to oceanic uptake implies that constraining the Southern Ocean flux is essential to constraining the global oceanic uptake of anthropogenic CO_2 . Likewise, understanding the dynamics of the future evolution of the Southern Ocean uptake is essential to understanding the total future oceanic uptake.

Simulations of the future climate show that the Southern Ocean will continue to play a key role in anthropogenic CO_2 uptake and that, given continuing emissions of CO_2 , the uptake in the region will continue to grow [10,11]. The rate of increase, however, will be subjected to known

processes, such as changes in the Revelle factor, and unknown processes, including the effects of climate change. Future climatic changes may alter the balance between circulation, stratification and biological production in the Southern Ocean and decrease the future uptake of anthropogenic CO₂ [12]. In order for us to distinguish interannual and decadal variability from secular trends, we must understand how these processes interact and have sufficient observations to inform our understanding at the process level.

Autonomous floats provide a powerful complement to shipboard measurements by routinely sampling profiles at high temporal density. The ARGO programme has been a substantial new data source about the global ocean since its deployment, including in the Southern Ocean [13]. Recent advances in float-based measurement platforms make it possible to equip floats with sensors of pH, nutrients and oxygen [14]. When combined with inverse methods and data assimilation, such floats can provide both improved state estimates and constraints for process-based models of the carbon system and ocean biogeochemistry. In this paper, we evaluate how effective such a system might be in resolving the Southern Ocean CO₂ flux for monthly and annual averages, and long-term trends.

Here, we review model and empirical estimates for CO₂ uptake in the Southern Ocean, how it may respond to climate change and the difficulties imposed by the sparse measurements in the region. We use an observational system simulation experiment (OSSE) to discuss float-based sampling benefits and strategies. This experiment complements a previous analysis, which showed that a float-based sampling with three-monthly sampling of $3 \times 30^\circ$ latitude–longitude resolution could achieve annually averaged Southern Ocean flux estimates with acceptable error [15].

2. Review of Southern Ocean carbon dioxide uptake

The global oceanic uptake of anthropogenic CO₂ and natural CO₂ depends strongly on the uptake that takes place in the Southern Ocean. Here, we demonstrate that the Southern Ocean is the primary source of uncertainty in the global oceanic uptake for a recent decade (1995–2005) and that the Southern Ocean plays a substantial part in setting the sensitivity of the CO₂ uptake to climate change. We consider examples from the literature and present model results for CO₂ uptake. Model results from phase 5 of the Coupled Model Intercomparison Project (CMIP5) are included [3,16], featuring 12 climate–carbon cycle models. These simulations were previously analysed to compare the ability of the current-generation coupled climate models to simulate the uptake of anthropogenic CO₂ and excess heat [3]. For comparison, ocean–biogeochemistry simulations are included based on the NOAA-GFDL (Geophysical Fluid Dynamics Laboratory) MOM4p1 model [17], coupled to the biogeochemistry model BLING (biology, light, iron, nutrient and gases) [18]. These simulations were forced at the ocean surface with three different atmospheric reanalysis products: NCEP-1 [19], CORE-II [20] and ERA-40 [21]. Each set of simulations has a ‘historical’ case, where the biogeochemical model feels the historical increase in atmospheric CO₂ such that the oceans are a net sink of CO₂ from the atmosphere, and a ‘preindustrial’ case, where atmospheric CO₂ concentrations are held constant at preindustrial values.

Anthropogenic CO₂ uptake is calculated as the difference between the fluxes from the ‘historical’ and ‘preindustrial’ simulations from both the CMIP5 and MOM4p1–BLING ensembles. The flux calculated directly from the ‘historical’ simulations is called the total or contemporary flux. The contemporary CO₂ flux is the sum of the natural and anthropogenic CO₂ fluxes. For purposes of comparison, we include data-based estimates of the anthropogenic and contemporary CO₂ fluxes. The estimates of the anthropogenic CO₂ uptake come from an inversion of ocean interior measurements [22]. The contemporary uptake estimates come from inversions of *p*CO₂ data. We use both the Lamont–Doherty Earth Observatory (LDEO) climatology [5], centred on the year 2000, and a reconstruction of historical *p*CO₂ from 1980–2009 (Markov chain Monte Carlo (MCMC) *p*CO₂ history) [23].

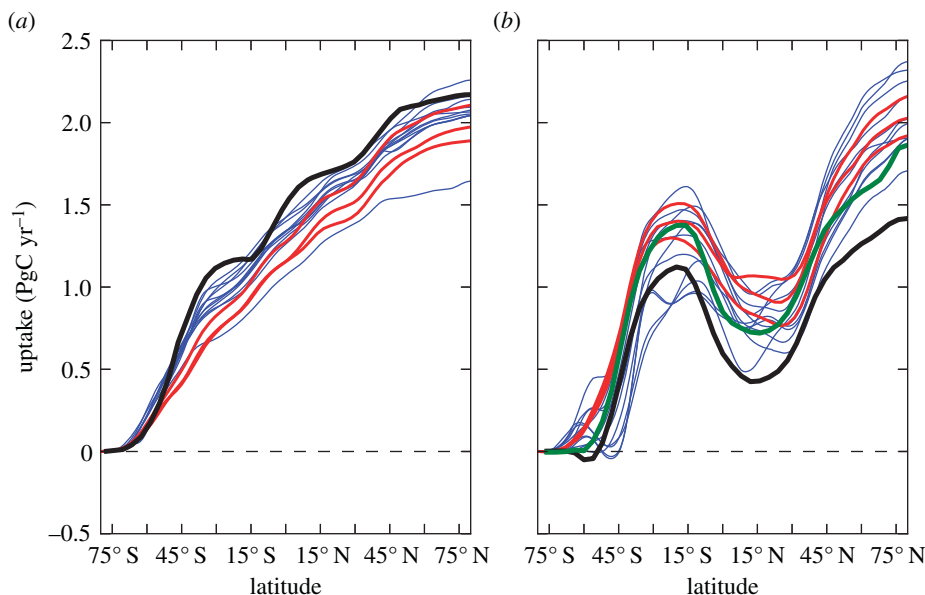


Figure 2. The cumulative fluxes integrated from 90° S to 90° N, in PgC yr⁻¹, of (a) anthropogenic CO₂ and (b) total CO₂. Estimates come from forced (red) and coupled (blue) oceanic GCMs averaged over 1995–2005 and show significant spread by 30° S. The black line in (a) shows the oceanic inversion results from Mikaloff Fletcher *et al.* [22]. In (b), the LDEO *p*CO₂ year 2000 climatological flux is in black and the MCMC *p*CO₂ history, averaged over 1995–2005, is in green.

(a) Decadal estimates

Recent model simulations indicate that the Southern Ocean (beyond 30° S) anthropogenic CO₂ uptake was 0.8 ± 0.1 PgC yr⁻¹ [3], for the decade 1995–2005, with a range defined by the red and blue lines in figure 2a. In that decade, the Southern Ocean uptake constituted 40–50% of the global total in the modelled fluxes. Empirical estimates from oceanic inversion give the uptake to be 1.1 PgC yr⁻¹ (52% of the global total) for the same region and decade (cf. black line in figure 2a) [22]. The reduced uptake in the suite of models is consistent with the whole of the CMIP5 historical simulations, which show less oceanic uptake of CO₂ than empirical studies [24]. Poor simulation of the stratification in the Southern Ocean is a suspected source of the underestimated anthropogenic uptake [3]. The proportion of anthropogenic CO₂ that enters through the Southern Ocean appears to be stable through time, with historical estimates of the total uptake indicating that about 50% of oceanic anthropogenic CO₂ entered through the Southern Ocean [25].

The estimates of the contemporary CO₂ uptake vary across a larger range than the anthropogenic uptake. The estimates of the northward cumulative flux of contemporary CO₂ span 1.1 ± 0.2 PgC yr⁻¹ at 30° S (shown in figure 2b). The total range in the estimates is set by the CMIP5 historical simulations (shown in blue lines in figure 2b). The MOM4p1–BLING simulations show slightly higher uptake, ranging between 1.2 and 1.4 PgC yr⁻¹ (red lines in figure 2b). The empirical estimate based on the MCMC *p*CO₂ history gives 1.3 ± 0.3 PgC yr⁻¹ (green line in figure 2b) and the LDEO climatology gives 1.0 ± 0.2 PgC yr⁻¹ (black line in figure 2b). The full spread in the CMIP5 estimates of contemporary uptake reveals significant uncertainty in the CO₂ flux as simulated by that ensemble. In some of the models, the Southern Ocean is not a sink of CO₂ south of 45° S, which betrays significant process-based errors. The northward cumulative plots in figure 2 show that the uncertainty in the total global uptake is established by 30° S, and thus the Southern Ocean is critical to the estimates of both the global mean and the uncertainty in CO₂ uptake.

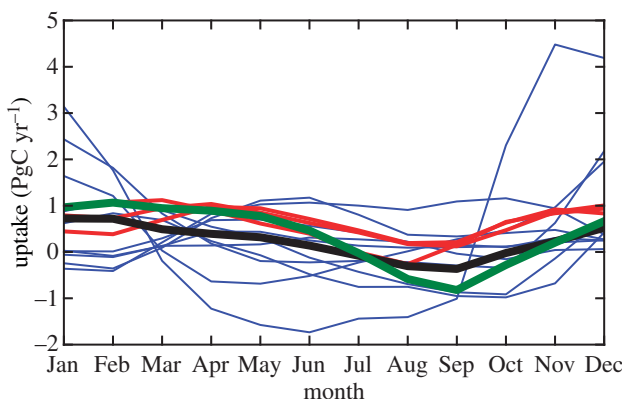


Figure 3. The seasonal cycle of CO_2 uptake into the Southern Ocean, south of 45°S , in PgC yr^{-1} . The CMIP5 models are shown in blue, MOM4p1-BLING models in red, the LDEO $p\text{CO}_2$ climatology in black and the MCMC $p\text{CO}_2$ history in green. The area south of 45°S was chosen to avoid contaminating the seasonal cycle with subtropical signals.

The seasonal cycle is considered for uptake south of 45°S in figure 3. The observationally derived uptake in the summer and autumn is driven by biological uptake and surface stratification. In the winter, deep mixed layers and the associated upwelling CO_2 drive weakened uptake or outgassing [5] (cf. black and green lines in figure 3). In CMIP5, the range in monthly estimates is quite large over the annual cycle, and those models do not demonstrate a clear seasonal cycle (blue lines in figure 3) [26]. The MOM4p1-BLING simulations (red lines in figure 3) show reasonable agreement with the empirically derived seasonal cycles, though the magnitude of the seasonal cycle is smaller in the model. The CMIP5 models, however, are inconsistent and many vary widely from the observationally based estimates. The seasonal amplitude of the fluxes in the CMIP5 models is particularly large compared with the observationally based estimates, in opposition to what happens with the forced models.

Reproducing the seasonal cycle of CO_2 fluxes in the Southern Ocean clearly poses a particular challenge for models. In forced ocean models, resolving the mixed layer depths, and thus the entrainment and export of dissolved inorganic carbon (DIC) from the surface, is vital to capturing the seasonal cycle in CO_2 fluxes [27]. Most forced models miss winter outgassing because of poor mixed layer simulation, including the MOM4p1-BLING simulations. These errors seem enhanced in the CMIP5 models, which have a wide variety of mixed layer characteristics but are generally too shallow [28]. However, the relative contributions of biological processes are yet to be determined, as the parametrization of co-limitation by temperature, light and micronutrients can also have a significant impact on the seasonal cycle [29–31].

The paucity of measurements makes empirical analysis of the seasonal cycle difficult. Analysis of surface $p\text{CO}_2$ measurements provides the most information about the seasonal flux of CO_2 over several decades. The sampling that is available for surface $p\text{CO}_2$ in the newly released Surface Ocean CO_2 Atlas (SOCAT) database [32,33], similar in nature to that which was used to make the climatology [5], is shown in figure 1. It shows that the seasonal cycle is resolved only in limited parts of the Southern Ocean and that there is a strong bias towards summer sampling. The lack of measurements limits the ability of the data to constrain the seasonal fluxes. For instance, the two $p\text{CO}_2$ data products shown in figures 2b and 3 use the same surface $p\text{CO}_2$ dataset [34] to calculate the air–sea CO_2 flux, yet the fluxes from the MCMC $p\text{CO}_2$ history express a higher-amplitude seasonal cycle than the LDEO climatology. Meanwhile, they are not distinguishable with the observations, with root mean squared error (RMSE) against the data of 20.6 (MCMC history) and 23.7 (climatology). The disagreement between the two occurs in regions and months where there is little or no data, and is created by differences in the spatial interpolation schemes, representation of the seasonal cycle and interannual variability [23]. The difference between the estimates projects into the overall carbon budget, where the available measurements cannot

separate the estimates of the CO_2 flux that are different by 0.3 PgC yr^{-1} or nearly 30% of the total Southern Ocean uptake.

(b) Southern Ocean carbon–climate feedbacks

Ocean circulation and mixing changes induced by global warming might affect the CO_2 uptake through several mechanisms. Wind-driven increased upwelling of CO_2 -rich deep waters may result in increased outgassing of natural CO_2 if biological production does not balance the increased supply of DIC [35]. These wind-driven changes are closely related to changes in the Southern annular mode (SAM) [36]. However, increases in stratification due to changes in sea ice or precipitation at high latitudes may oppose the wind-driven changes via a reduction of natural outgassing south of the ACC [12]. In addition, thermal solubility effects may reduce the ability of the surface to capture CO_2 from the atmosphere [12]. The potential impact of climate change on the Southern Ocean CO_2 uptake is difficult to anticipate because of the varying balances between biology and ocean circulation that govern the Southern Ocean CO_2 uptake.

The impact of climate is estimated by calculating the difference in the CO_2 uptake between model runs with and without climate change, but with increasing atmospheric CO_2 concentrations. Current coupled modelling efforts indicate that the Southern Ocean CO_2 flux may have already decreased owing to changes in the climate, relative to model simulations where climate is held constant, but that the impact is currently small [3]. Northward cumulative climate impacts indicate that climate signals decreased the modelled CO_2 uptake in the Southern Ocean between 1970 and 2005 by $2\text{--}3 \text{ PgC}$ (cf. figure 4b). That decrease in uptake holds in five of the seven simulations.

The picture of reduced uptake in the past few decades, relative to what might be expected in the absence of climate change, holds across forced and coupled models and the empirical estimates. Figure 4b shows the northward cumulative climate impact from the CMIP5 and MOM4p1–BLING models integrated from 1970 to 2005. A negative value in the cumulative plots indicates where the effect of climate has been to decrease the oceanic sink. The preponderance of negative values at 30°S illustrates the role of the Southern Ocean in establishing the climate impacts from figure 4a.

Recent joint studies of ocean model simulations and atmospheric inversions introduced the hypothesis that changes in the Southern Ocean CO_2 uptake are already occurring [37]. They proposed that increases in the wind stress (positive SAM) over the Southern Ocean had decreased the uptake of CO_2 into the Southern Ocean by $-0.08 \text{ PgC yr}^{-1} \text{ decade}^{-1}$ between 1981 and 2004 (approx. -2 PgC total) relative to what the uptake would have been had there been no change to the ocean circulation. *In situ* observations support the hypothesis that surface carbon has been increasing [38], though it is unclear whether that has been expressed as a decreasing flux for the whole ocean [23]. Evidence from chlorofluorocarbon measurements suggests that the Southern Ocean has recently displayed substantial ventilation increases [39].

Ocean biogeochemical models support this hypothesis, but show to varying extents that the mechanism is reduced by alkalinity-driven solubility changes [40] and enhanced biology [41,42] responding to increased upwelled nutrient levels [43]. In addition, the coarse resolution used in these ocean modelling studies means that the predicted reduction of the carbon uptake may have been overestimated compared with models with improved eddy representation (or what we might expect in the real ocean) [41,44,45]. However, the exact sensitivity of the carbon flux to changing winds is not well constrained. It is likely that wind-driven changes in the circulation have dominated the climate change impact on the carbon uptake in recent decades, as stratification changes in the higher latitudes are only just beginning [46].

3. Float-based sampling experiment

Increased observational density in space and time should enhance our ability to monitor the Southern Ocean CO_2 uptake and to constrain models of the processes that drive uptake and

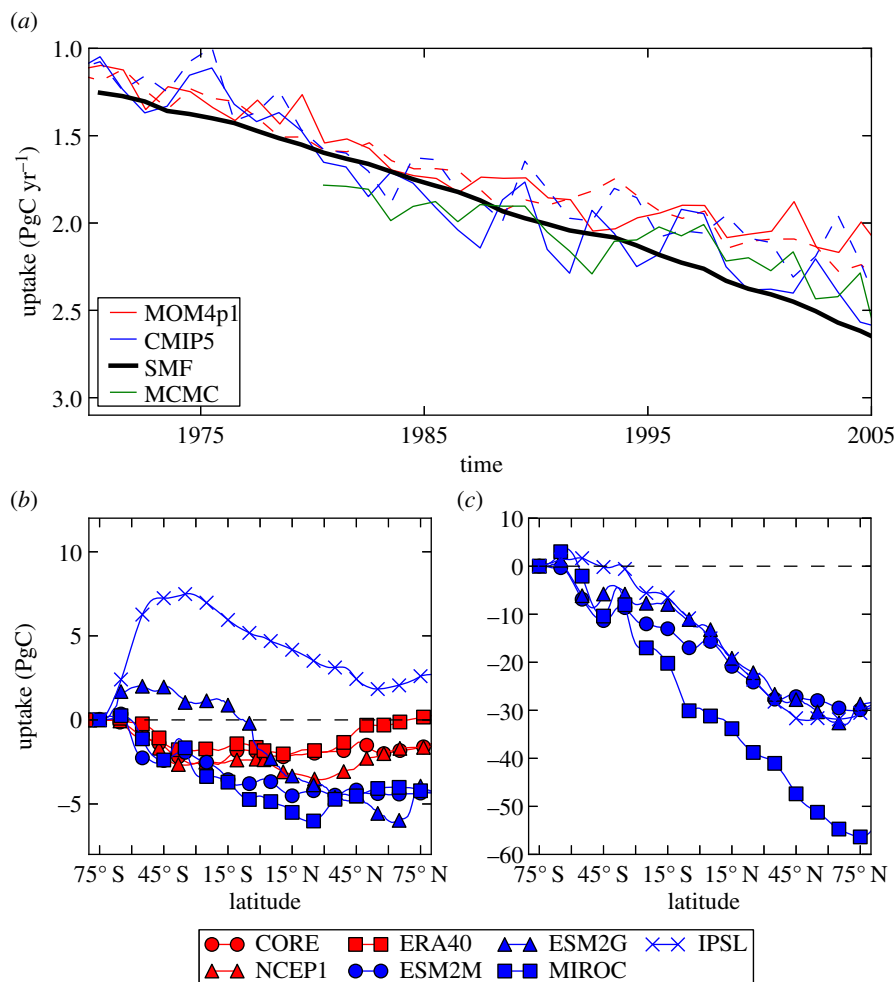


Figure 4. (a) The impact of climate change on the total global ocean CO₂ uptake between 1970 and 2005. The time series show the uptake of CO₂, with (dashed) and without (solid) climate variability, by the ocean from CMIP5 (blue) and MOM4p1–BLING simulations (red). The MCMC uptake is shown in green, and an extrapolation of the Mikaloff Fletcher inversion is shown in solid black. (b) The climate impact on CO₂ uptake, in PgC, integrated over 1970–2005 and northward from 90° S for each model. (c) The climate impact on CO₂ uptake, in PgC, integrated over 1860–2100 and northward from 90° S for the RCP4.5 simulations.

its response to global warming. A simple OSSE is used here to evaluate the effectiveness of a float-based sampling programme for estimating the basin-scale CO₂ flux in the Southern Ocean (beyond 30° S) and monitoring it for trends and changes. The OSSE generates a synthetic sampling from model output and attempts to reconstruct the modelled fields from the simulated data.

The GFDL-ESM2M ‘historical’ simulation (years 1995–2000) [47] is used as the ‘true’ case from which the synthetic sampling is produced. The sampling points are randomly distributed across the area of the Southern Ocean south of 30° S (cf. figure 5). The simulated floats do not move horizontally and sample the surface CO₂ flux from the model grid cell that they occupy monthly. The lack of horizontal movement, which should occur passively with the flow, may add some bias to the reconstruction, but the effect of movement in reconstructing physical parameters in other OSSEs has been quantified [48]. The monthly sampling produces a set of 60 individual samples, X_i^{model} , for each of the N floats. The value of N is 200 in the base case, as shown in figure 5, but a range of values from 100 to 500 is explored.

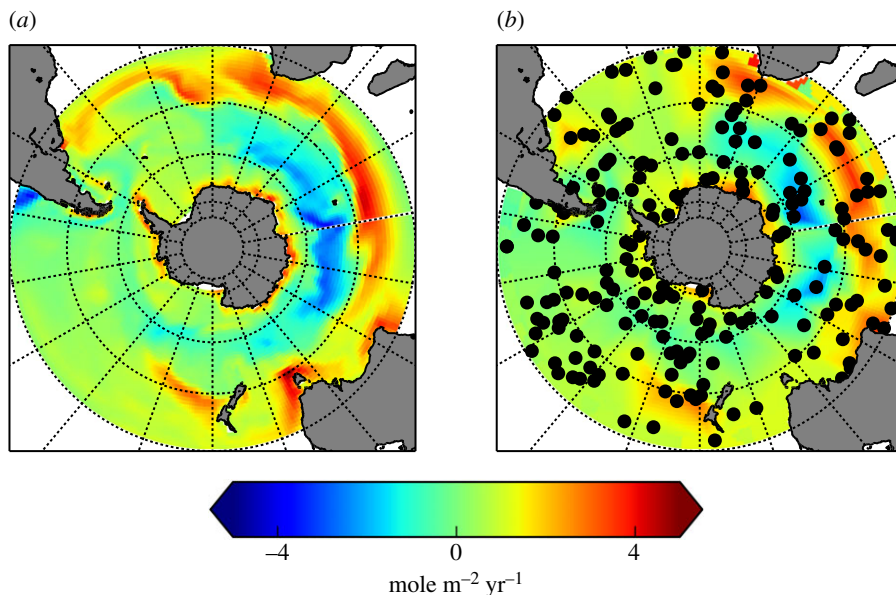


Figure 5. The modelled annual flux, in $\text{mole m}^{-2} \text{yr}^{-1}$, from the ESM2M historical simulation is shown as calculated (a) directly on the fully sampled model grid and (b) using 200 randomly distributed and stationary floats with a 20% sampling error. The true flux for the year was 0.79 PgC, and the reconstruction shown here results in a flux of 0.76 PgC.

Random fluctuations are added to the direct samples, X_i^{model} , to model instrumental error and because the coarse resolution of the model grid and the monthly sampling do not represent the variability present in real point surface measurements. The sources of likely variability include: effects of mesoscale eddies, synoptic variability in the surface fields, analytical error in inverting the carbon system, and instrumental error. The error is imposed by adding deviations to the sampled model values. The deviations are modelled as uncorrelated normal random variables with standard deviations equal to a percentage of the true value, i.e. $\text{std}(X'_i) = \epsilon X_i^{\text{model}}$. The synthetic samples include this fractional error, such that $X_i = X_i^{\text{model}} + X'_i$.

The scale of the error term, ϵ , that would be expected in real observations is not known. Estimates of the air–sea CO_2 flux from float data must involve an inversion of the surface carbonate chemistry to $p\text{CO}_2$, from two of pH, DIC and alkalinity. Alkalinity can be estimated from diagnostic relationships with salinity, temperature and depth with reasonable precision ($\pm 8.4 \mu\text{mol kg}^{-1}$) [49]. Low-power pH sensors, for deployment on floats and moorings, are currently in development [50]. Mooring-based instruments for pH have achieved estimates of $p\text{CO}_2$, inverted using salinity-estimated alkalinity and pH measurements, of $\pm 13 \mu\text{atm}$ over two-month deployments, but suffer some drift [51]. This work assumes that pH-instrumented floats will be available with similar precision and drift correction in the near future. Given the coarse resolution of the model field, eddy effects would also need to be taken into account, though along-track $p\text{CO}_2$ observations indicate that this is a small effect and adds an error of about $3 \mu\text{atm}$ [15]. While these sources of error should not be discounted, it is assumed that the gas exchange parametrization error will be dominant in achieving local flux estimates from point measurements. The expected precision of inverted $p\text{CO}_2$ and the effects of eddies would be between 1% and 3% of an average Southern Ocean $p\text{CO}_2$ of $340 \mu\text{atm}$; smaller than the uncertainties associated with gas exchange piston velocity [5]. Thus, a fractional sampling error of 20% is assumed for the base case presented here, because this is the error associated with the parametrization associated with gas exchange. This level of error assumes that the other error sources are small and potentially compensating, but a range of fractional errors from 0.0 to 0.5 are explored to examine the robustness of the results to a range of inverted $p\text{CO}_2$ precisions.

The simulated samples X_i are projected back onto the model grid using simple objective mapping with inverse distance scaling. The gridded values then constitute the reconstructed CO₂ flux for each month (cf. figure 5b). The error induced by the mapping and carried through from the error added to the samples negatively affects the accuracy of the reconstructed CO₂ flux. The error in the basin-scale CO₂ uptake estimate is found via bootstrapping from a Monte Carlo simulation for each combination of (N, ϵ) . The Monte Carlo simulation consists of 1000 simulated samplings, each with an individual distribution of the simulated floats. The error in the reconstructions is estimated using the standard deviation across the 1000 members of the Monte Carlo simulation.

The ability of the sampling strategies to capture trends in the basin-scale CO₂ flux is assessed using the bootstrapped error estimates and the autocorrelation in the time series of the modelled uptake. The calculation of the minimum amplitude detectable is carried out according to the relationship in equation (3.1) [52], between the number of years of monthly estimates n , the error in the monthly estimates σ and the autocorrelation in the time series ϕ :

$$\min|A| = \frac{3.3\sigma_N}{n^{3/2}} \sqrt{\frac{1+\phi}{1-\phi}}. \quad (3.1)$$

Equation (3.1) shows that the minimum detectable trend increases with the size of the noise in the data and with the level of autocorrelation in the time series. The dependence on autocorrelation is quite important to this analysis, as it increases the time necessary to detect a trend of a certain magnitude. For a fixed period of observation, a moderate autocorrelation of $\phi = 0.5$ will increase the size of the minimum detectable trend by a factor of 1.73. The GFDL-ESM2M ‘historical’ simulation’s Southern Ocean CO₂ annual uptake has an autocorrelation of 0.5. Thus, it plays an important part in evaluating the ability of the repeated observation to detect a trend. The bootstrapped error in the monthly reconstructions is also an important input for the trend detection.

(a) Estimates

The reconstructed fluxes capture the total Southern Ocean uptake (south of 30° S) and the large-scale structures in the flux field. One example of the reconstructed flux, averaged for the year 2000, is shown in figure 5 for the base case sampling with 200 floats. While the sampling in the base case is still sparse, the reconstruction is capable of resolving many features of the flux field because of the zonal nature of the Southern Ocean and the large-scale features in the coarse-model flux field [15]. Here, we assess the skill of the reconstructed fluxes to capture the total uptake of CO₂ at the basin scale and the patterns of variability within the Southern Ocean.

Capturing the total uptake of CO₂ with high precision is an important task for constraining the global carbon budget. In the example shown in figure 5, the total uptake is 0.79 PgC yr⁻¹, which differs by 0.03 PgC yr⁻¹ error from the true modelled value of 0.76 PgC yr⁻¹. Monte Carlo simulation provides context to the error in that instance. In a simulation with 1000 arrangements of the 200 floats, the bootstrapped error of the year-to-year estimates (measured by standard deviation) is 0.07 PgC yr⁻¹. The total uptake in the example is thus consistent with the true flux within the bootstrapped error estimate.

We find that the reconstructed fluxes capture the true value of the annual uptake within the bootstrapped precision for the 5 years of the considered simulation. The annual fluxes for the 5 years of reconstruction and the model are shown in figure 6a. There, the $\pm 1\sigma$ range of the mean estimates (blue lines) contains the true annual values (black lines) from the model and separates the higher uptake in model years 1999 and 2000 from the earlier years. Thus, the base case sampling is capable of capturing the year-to-year Southern Ocean CO₂ uptake with enough precision to resolve interannual variability and to constrain and monitor Southern Ocean CO₂ uptake.

The monthly estimates of the total CO₂ uptake from the float-based sampling constrain the seasonal cycle in total uptake. The estimated error for the month-to-month fluxes is 0.1 PgC yr⁻¹, and monthly reconstructions are also successful in capturing the monthly flux, within the $\pm 1\sigma$

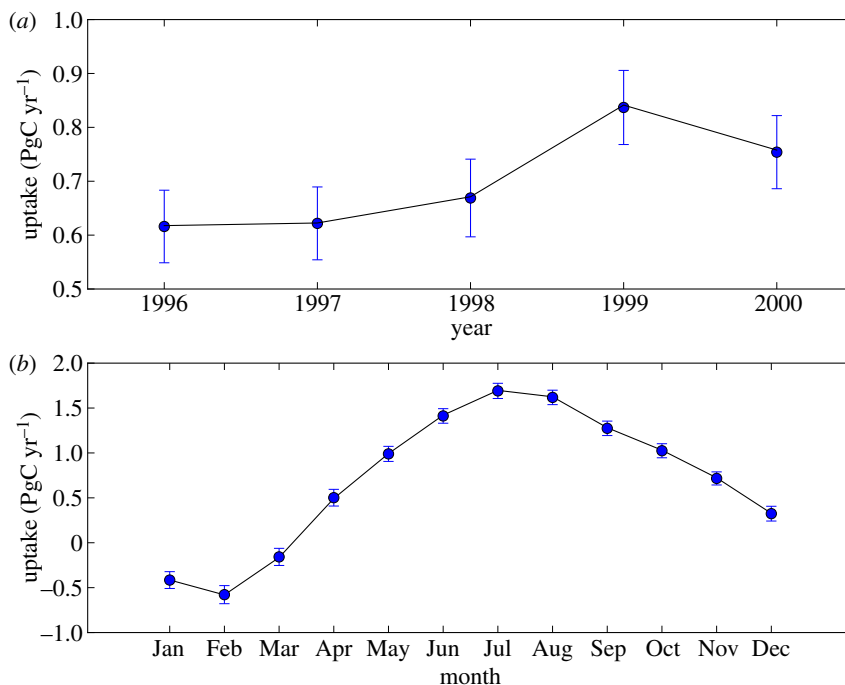


Figure 6. The annual reconstruction of the Southern Ocean CO₂ uptake, in PgC yr⁻¹, from the ESM2M historical simulation years over the period from 1996 to 2000 (a) and the averaged monthly uptake values for the 5 year reconstruction (b). The black line connects the true values of the flux. The blue bars show the $\pm 1\sigma$ uncertainty for each estimate, based on a 1000-member Monte Carlo simulation of 200 floats with 20% fractional sampling error.

bands, of the mean estimate from the Monte Carlo simulation (cf. figure 6b). Note that the seasonal cycle in uptake south of 30° S, as shown in figure 6b, is different from the region south of 45° S, as was shown in figure 3. However, the simulated sampling retrieves the seasonal cycle in the smaller domain as well.

(b) Trend detection

The bootstrapped error for the monthly uptake estimate contributes to the calculation of the minimum detectable trend via equation (3.1). The calculation also relies on the lag-1 autocorrelation in the CO₂ uptake from the ESM2M simulation. The autocorrelation is set at the modelled value of 0.5, and the monthly error in the uptake estimate is 0.07 PgC yr⁻¹. The magnitude of the minimum detectable trend (90% significance level) is shown in figure 7. The magnitude of the minimum detectable trend decreases quickly with the number of years of continuous monthly observations and asymptotes towards very small trends after 40 years.

The detection of the trends associated with the continued uptake of CO₂ in the Southern Ocean and the response of the circulation to climate change from models is important. Based on the scenario projections from the CMIP5 simulations discussed in §2, we can calculate that the uptake of continued CO₂ emissions to the atmosphere will drive an increasing trend in the Southern Ocean CO₂ uptake of 0.2 PgC yr⁻¹ decade⁻¹. Changes to that background trend due to the potential impacts of climate change have an unknown magnitude. Thus, we focus on detecting a trend magnitude of the same size as the one associated with recent saturation of the Southern Ocean CO₂ sink, which is equivalent to a decadal change of $-0.08 \text{ PgC yr}^{-1} \text{ decade}^{-1}$ [37]. Inverting the detection limits in figure 7, we find that the trend from continued growth of the

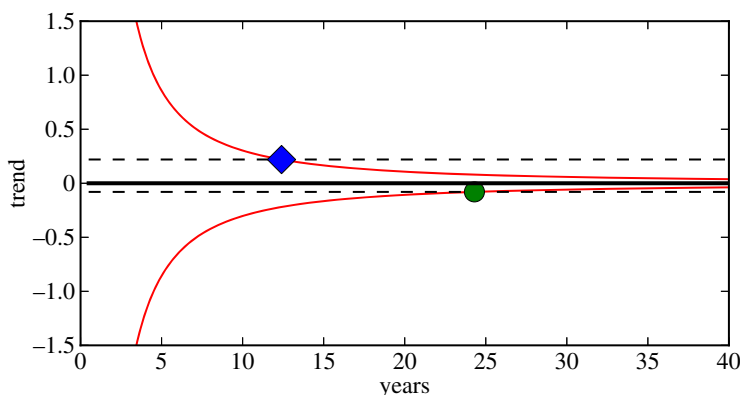


Figure 7. Minimum detectable trend (red lines), in $\text{PgC yr}^{-1} \text{ decade}^{-1}$, is a function of the number of years of monthly sampling, the error in the monthly estimates and the autocorrelation in the time series of uptake. Fifteen years of continuous monthly sampling are required to capture the historical trend associated with the uptake of anthropogenic CO_2 in the Southern Ocean (blue diamond, $0.2 \text{ PgC yr}^{-1} \text{ decade}^{-1}$). More than 20 years are required to capture a trend with the magnitude expected from changes in the overturning circulation (green circle, $-0.08 \text{ PgC yr}^{-1} \text{ decade}^{-1}$).

Southern Ocean CO_2 sink would take 13 years to detect, and the reduction due to climate would require 24 years of continuous monthly measurements.

(c) Sensitivity studies

The robustness of the reconstructions to the size of the sampling array and the error associated with the individual measurements is assessed via a sensitivity study. Here, the number of floats is varied between (50, 500) and the fractional sampling error varies over (0.0, 0.5). For each pair of parameters, we use the same method of simulating the observations as previously outlined and use a 1000-member Monte Carlo simulation to estimate the errors associated with the reconstruction process. The reconstructions are examined for both the total integral error, associated with uptake estimates for the Southern Ocean, and resolution of the local fluxes. For the latter, we measure the percentage of reconstructed cells, on the GFDL-ESM2M model grid, where the bootstrapped error estimate is larger than a threshold value of $1 \text{ mole m}^{-2} \text{ yr}^{-1}$. The threshold level of $1 \text{ mole m}^{-2} \text{ yr}^{-1}$ is small enough to resolve the local seasonal cycle over 99% of the Southern Ocean area in the ESM2M simulation. The two measures evaluate the potential contribution of varying sampling arrays to monitoring Southern Ocean uptake and the flux variability within the Southern Ocean.

We chose the percentage of exceedance as a metric of the fidelity of the reconstructions, because it provides a basin-wide estimate of the ability of the reconstructed fluxes to re-create spatio-temporal variability of the Southern Ocean CO_2 uptake. The fidelity of the reconstructions at the local scale will define their usefulness for examining the process-based questions that result in the high degree of uncertainty in the uptake estimates and projections. Examples of the exceedance percentage for float arrays with 75, 200 and 400 samplers indicate that large areas within the Southern Ocean will be resolved for the more moderate sampling (cf. figure 8). Nevertheless, higher numbers of floats decrease the areas with error exceeding the threshold by nearly 20% of the Southern Ocean area. The high-sampling cases leave only coastal and boundary regions where the precision of the reconstruction is above this threshold throughout the year.

The number of floats strongly influences the ability of the float-based sampling to capture both the integral error and the local fluxes with high precision. The estimated error of the monthly basin uptake goes from more than 0.2 PgC yr^{-1} to less than 0.05 PgC yr^{-1} between 50 and 500 floats, with a strong drop-off in the error estimate occurring before 200 floats (cf. figure 9). The

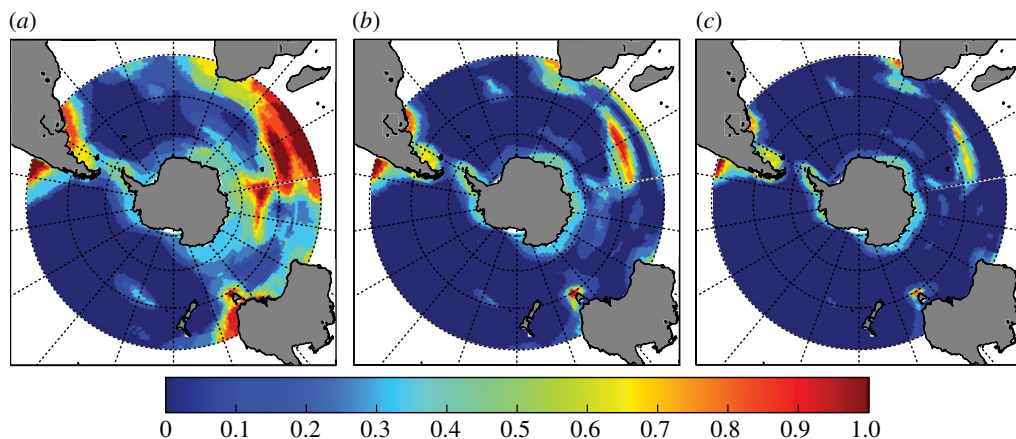


Figure 8. The proportion of months for which the bootstrapped error estimate is larger than the threshold value of $1 \text{ mole m}^{-2} \text{ yr}^{-1}$. The area of exceedance decreases from samplings with 75 (a), 200 (b) and 400 (c) floats. The bootstrapped errors come from the 1000-member Monte Carlo simulation for each number of floats.

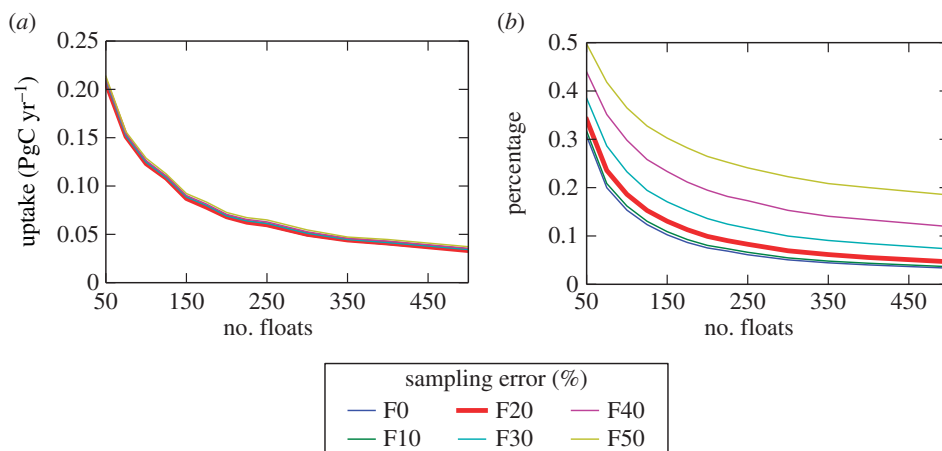


Figure 9. (a) Error estimates for the annual reconstruction of the Southern Ocean CO_2 uptake, in PgC , for varying number of floats. The error estimates are calculated as the standard deviation of the basin-integrated annual CO_2 flux from the reconstructed fields and the true model. (b) The percentage of the Southern Ocean, south of 30° S , where the monthly error estimate is larger than the threshold value of $1 \text{ mole m}^{-2} \text{ yr}^{-1}$. In both plots, different lines reflect reconstructions with varying levels of sampling error. The error in the estimate of total uptake is less sensitive to the sampling error than the percentage of exceedance.

same drop-off is present in the percentage area of exceedance. For the fractional sampling error of 20%, the area of exceedance falls from 34% to 9% between 50 and 200 floats. It falls to 4% with 500 floats. Again, the percentage exceedance asymptotes with more floats, such that there are diminishing returns for numbers of floats increasing beyond 200.

The sensitivity of the percentage of exceedance to the scale of the sampling error is much larger than that for the total uptake. The curves in figure 9 show the relationship for the integral error and percentage exceedance against the number of floats. In the case of integral error, the error estimates vary little with the scale of the sampling error compared with the difference across the number of floats. By contrast, the percentage area of exceedance is as sensitive to the fractional sampling error as it is to the number of floats over the ranges tested for each. The low-high

estimates for the percentage exceedance are (30%, 50%) for simulations with 50 floats and (4%, 18%) for simulations with 500 floats (cf. figure 9) for the fractional sampling errors that vary from 0% to 50% imposed error.

4. Discussion

The results from the OSSE presented here indicate that a float-based measurement system should be able to resolve the Southern Ocean CO₂ flux with a greater level of certainty than current methods. Current measurement density allows for a substantial difference in decadal empirical estimates of the CO₂ uptake, 0.3 PgC yr⁻¹, with an even larger spread in model behaviour (cf. figure 2). Reducing the empirical uncertainty in the monthly and annual CO₂ fluxes to 0.07 and 0.1 PgC yr⁻¹ should be possible with a float-based sampling at a scale of 150–200 floats. Such a system would be able to represent both the seasonal cycle and the annual mean uptake, which would provide a major constraint for atmospheric inversions [27] and studies of the ocean's role in the global carbon cycle [53].

Previous studies have considered the number of surface measurements that are necessary to capture the CO₂ flux at monthly and annual scales. Samplings with a density of 3° latitude and 30° longitude have been proposed as sufficient to resolve the annual Southern Ocean uptake [15]. Such a sampling density is similar to the base case that we investigated, with a density of one float per 95 square degrees on the ESM2M model grid. This study shows that, for the number of floats above 150–200, the ability to resolve both the monthly uptake and the local fluxes stops increasing, even when the floats are randomly distributed. This is most likely a result of the average decorrelation length scale in the coarse resolution models being resolved with 150–200 samplers [15]. It is still unknown how well the coarse ocean model that forms the basis of this study resolves the statistics and dependences of the CO₂ flux from the real ocean. Similar studies with high-resolution models might provide some additional information about the scales of variability that the floats must sample to generate suitable flux reconstructions. Future studies with high-resolution models might also give some indication of the actual size of the fractional sampling error due to variability that is not resolved by the 1° model that we used and provide benchmarks for the statistical upscaling of subgrid-scale variability.

The ability to capture trends in the CO₂ uptake in the Southern Ocean is limited by the error in the monthly estimates of the uptake, the month-to-month variability and the autocorrelation in the time series of uptake. The increased uptake from increasing atmospheric CO₂ will take a decade or slightly more to detect. The time to capture departures from such an expected trend, from changes associated with climate change, for instance, will take decades or more. Directly detecting changes in the Southern Ocean CO₂ uptake, such as the decrease of $-0.08 \text{ PgC yr}^{-1} \text{ decade}^{-1}$ associated with changes in wind stress [37], will take up to three decades. The smaller changes expected from reduced future uptake in the CMIP5-type models ($-0.02 \text{ PgC yr}^{-1} \text{ decade}^{-1}$; cf. figure 4c) will require 60 or more years of continuous observations. While the changes to the carbon uptake that are currently projected are hard to detect, mainly owing to the effects of autocorrelation and monthly variability, an updating flux estimate will provide some ability to measure large, unexpected, changes to the CO₂ uptake at the decadal scale (up to $0.3 \text{ PgC yr}^{-1} \text{ decade}^{-1}$ or half of the current uptake).

The synthetic sampling that we present here is an idealized case, which was meant to show how many measurements and what precision of measurement were needed to understand seasonal and year-to-year variations in the Southern Ocean CO₂ uptake. Continued effort should be expended to evaluate float-based sampling strategies within data assimilation frameworks and OSSEs such as this one. Critically, transport of the floats by the mean flow and eddies may affect the basin-scale monitoring of CO₂ uptake and may invalidate the assumption of a random distribution that we have used. In a high-resolution OSSE, the strong currents of the Southern Ocean affected the sampling distribution of floats in the Indian Ocean [54]. While eddies enforce a more uniform sampling distribution [48], strategies for float release, parking depth, time between

profiles and ice avoidance will need to be critically evaluated for how they impact the information provided by the whole sampling array and target undersampled regions.

5. Conclusion

Empirical and model estimates indicate that the flux of CO₂ in the Southern Ocean is critical to the global carbon budget. Up to 50% of the anthropogenic CO₂ that is absorbed by the ocean is captured within the Southern Ocean. Moreover, a significant portion of the uncertainty in estimates of the global oceanic CO₂ uptake originates in the Southern Ocean, south of 30° S. This is true for both empirical and model-based estimates, where empirical estimates are limited by the lack of available data in the Southern Ocean and model estimates show significant differences across models at the process level. Increased observational density is necessary to resolve the uncertainty in the Southern Ocean CO₂ uptake and the process-level understanding of the dynamics that govern the Southern Ocean CO₂ flux.

We have shown that an observational programme based on 150–200 vertically profiling floats, which could estimate surface CO₂ flux, would offer significantly more information about the Southern Ocean CO₂ uptake than is currently available on monthly, annual and interannual time scales. Such a system would provide annual estimates of the Southern Ocean uptake with an error of less than 0.1 PgC yr⁻¹ or less than 20% of the current uptake in the Southern Ocean or 5% of global oceanic uptake. This would be an important tool for monitoring the uptake of anthropogenic CO₂ by the ocean and understanding and monitoring the global carbon budget. This is particularly important for the Southern Ocean, where changes in the flux due to the effects of climate change could be a significant portion of the carbon cycle's response to climate change.

Moreover, an observational programme featuring 150–200 sampling floats would provide much higher resolution of the CO₂ flux at local and monthly scales. For an assumed threshold of 1 mole m⁻² yr⁻¹ (to capture more than 90% of the seasonal cycle), this system will offer resolution of the CO₂ flux over 90% of the Southern Ocean every year. This resolution will provide an opportunity to dramatically improve process-based understanding of the Southern Ocean CO₂ flux to help address the balances between gas exchange, biological uptake, upwelling, and entrainment and detrainment at the base of the mixed layer. By offering dense information at the ocean surface, it would provide an important complement to monitoring strategies based on repeat hydrographic monitoring of carbon accumulation in the ocean interior. Those studies could provide a benchmark against which the carbon uptake inferred from the float array measurements could be evaluated.

This study has focused on the uncertainty in and constraints for the Southern Ocean CO₂ flux. The array network considered here could serve as a critical component of a larger integrated network, wherein the floats could be equipped to measure nutrients, temperature, salinity and other biogeochemically important quantities. Profiling floats are specifically valuable because they measure the water column to 2000 m and provide information for subsurface studies. The spatially diffuse and temporally consistent measurements from these floats could provide a bridge between sparse, high-precision, hydrographic measurements and very high-resolution satellite products to develop an integrated understanding of Southern Ocean biogeochemistry at many time scales. Ongoing work is devoted towards achieving such a monitoring system [55,56]. In the same way that 150–200 floats measuring surface CO₂ could dramatically improve our understanding of the CO₂ flux, these measurements could contribute to understanding and monitoring other aspects of the biogeochemical system in the Southern Ocean, which is critical to the global cycling of nutrients and the capture of excess heat due to climate change by the ocean. Much more than being a tool for CO₂ monitoring, measurements of this scale and nature would offer significant opportunity to monitor and understand the Southern Ocean's role in an evolving ocean.

Acknowledgements. The authors greatly appreciate the careful reading and commentary of two reviewers and the editor of this Theo Murphy Meeting Issue. Comments from Adele Morrison were also appreciated. This report

was prepared by J.D.M. under award NOAA-NA11OAR4310066 from the National Oceanic and Atmospheric Administration, US Department of Commerce. This report was prepared by J.L.S. and K.B.R. under award NOAA-NA08OAR4320752 from the National Oceanic and Atmospheric Administration, US Department of Commerce. The statements, findings, conclusions and recommendations are those of the author(s) and do not necessarily reflect the views of the National Oceanic and Atmospheric Administration, or the US Department of Commerce. This material is based upon work supported by the National Science Foundation under grant no. ANT-1040957. Any opinions, findings and conclusions or recommendations expressed in this material are those of the author(s) and do not necessarily reflect the views of the National Science Foundation.

Funding statement. B.R.C. was supported by NSF grant no. ANT-1040957. C.O.D. was supported by the US Department of Energy under contract no. DE-SC0006848. T.L.F. acknowledges support from the SNSF (Ambizione grant no. PZ00P2-142573).

References

1. Marshall J, Speer K. 2012 Closure of the meridional overturning circulation through Southern Ocean upwelling. *Nat. Geosci.* **5**, 171–180. (doi:10.1038/ngeo1391)
2. Sarmiento JL, Gruber N, Brzezinski MA, Dunne JP. 2004 High-latitude controls of thermocline nutrients and low latitude biological productivity. *Nature* **427**, 56–60. (doi:10.1038/nature02127)
3. Frölicher TL, Sarmiento JL, Paynter D, Dunne JP, Winton M. Submitted. Carbon and heat uptake in the CMIP5 models: the dominance of the Southern Ocean. *J. Clim.*
4. Gruber N *et al.* 2009 Oceanic sources, sinks, and transport of atmospheric CO₂. *Glob. Biogeochem. Cycles* **23**, GB1005. (doi:10.1029/2008GB003349)
5. Takahashi T *et al.* 2009 Climatological mean and decadal change in surface ocean pCO₂, and net sea–air CO₂ flux over the global oceans. *Deep Sea Res. II: Top. Stud. Oceanogr.* **56**, 554–577. (doi:10.1016/j.dsr2.2008.12.009)
6. Hallberg R, Gnanadesikan A. 2006 The role of eddies in determining the structure and response of the wind-driven southern hemisphere overturning: results from the Modeling Eddies in the Southern Ocean (MESO) project. *J. Phys. Oceanogr.* **36**, 2232–2252. (doi:10.1175/JPO2980.1)
7. Sabine CL *et al.* 2004 The oceanic sink for anthropogenic CO₂. *Science* **305**, 367–371. (doi:10.1126/science.1097403)
8. Caldeira K, Duffy PB. 2000 The role of the Southern Ocean in uptake and storage of anthropogenic carbon dioxide. *Science* **287**, 620–622. (doi:10.1126/science.287.5453.620)
9. Le Quéré C *et al.* 2009 Trends in the sources and sinks of carbon dioxide. *Nat. Geosci.* **2**, 831–836. (doi:10.1038/ngeo689)
10. Roy T *et al.* 2011 Regional impacts of climate change and atmospheric CO₂ on future ocean carbon uptake: a multimodel linear feedback analysis. *J. Clim.* **24**, 2300–2318. (doi:10.1175/2010JCLI3787.1)
11. Lovenduski NS, Ito T. 2009 The future evolution of the Southern Ocean CO₂ sink. *J. Mar. Res.* **67**, 597–617. (doi:10.1357/002224009791218832)
12. Sarmiento JL, Hughes TMC, Stouffer RJ, Manabe S. 1998 Simulated response of the ocean carbon cycle to anthropogenic climate warming. *Nature* **393**, 245–249. (doi:10.1038/30455)
13. Roemmich D, Johnson GC, Riser S, Davis R, Gilson J, Owens WB, Garzoli SL, Schmid C, Ignaszewski M. 2009 The Argo program: observing the global ocean with profiling floats. *Oceanography* **22**, 34–43. (doi:10.5670/oceanog.2009.36)
14. Johnson KS, Riser SC, Karl DM. 2010 Nitrate supply from deep to near-surface waters of the North Pacific subtropical gyre. *Nature* **465**, 1062–1065. (doi:10.1038/nature09170)
15. Lenton A, Matear RJ, Tilbrook B. 2006 Design of an observational strategy for quantifying the Southern Ocean uptake of CO₂. *Glob. Biogeochem. Cycles* **20**, GB4010. (doi:10.1029/2005GB002620)
16. Taylor KE, Stouffer RJ, Meehl GA. 2011 An overview of CMIP5 and the experiment design. *Bull. Am. Meteorol. Soc.* **93**, 485–498. (doi:10.1175/BAMS-D-11-00094.1)
17. Griffies SM, Harrison MJ, Pacanowski RC, Rosati A. 2004 A technical guide to MOM4. Available at <http://www.gfdl.noaa.gov/>.
18. Galbraith ED *et al.* 2011 Climate variability and radiocarbon in the CM2Mc Earth system model. *J. Clim.* **24**, 4230–4254. (doi:10.1175/2011JCLI3919.1)

19. Kalnay E *et al.* 1996 The NCEP/NCAR 40-year reanalysis project. *Bull. Am. Meteorol. Soc.* **77**, 437–471. (doi:10.1175/1520-0477(1996)077<0437:TNYRP>2.0.CO;2)
20. Large WG, Yeager SG. 2009 The global climatology of an interannually varying air–sea flux data set. *Clim. Dyn.* **33**, 341–364. (doi:10.1007/s00382-008-0441-3)
21. Uppala SM *et al.* 2005 The ERA-40 re-analysis. *Q. J. R. Meteorol. Soc.* **131**, 2961–3012. (doi:10.1256/qj.04.176)
22. Mikaloff Fletcher SE *et al.* 2006 Inverse estimates of anthropogenic CO₂ uptake, transport, and storage by the ocean. *Glob. Biogeochem. Cycles* **20**, GB2002. (doi:10.1029/2005GB002530)
23. Majkut JD, Sarmiento JL, Rodgers KB. 2014 A growing oceanic carbon uptake: results from an inversion study of surface pCO₂ data. *Glob. Biogeochem. Cycles* **28**. (doi:10.1002/2013GB004585)
24. Friedlingstein P, Meinshausen M, Arora VK, Jones CD, Anav A, Liddicoat SK, Knutti R. 2013 Uncertainties in CMIP5 climate projections due to carbon cycle feedbacks. *J. Clim.* **27**, 511–526. (doi:10.1175/JCLI-D-12-00579.1)
25. Khatiwala S, Primeau F, Hall T. 2009 Reconstruction of the history of anthropogenic CO₂ concentrations in the ocean. *Nature* **462**, 346–349. (doi:10.1038/nature08526)
26. Anav A *et al.* 2013 Evaluating the land and ocean components of the global carbon cycle in the CMIP5 Earth system models. *J. Clim.* **26**, 6801–6843. (doi:10.1175/JCLI-D-12-00417.1)
27. Lenton A *et al.* 2013 Sea–air CO₂ fluxes in the Southern Ocean for the period 1990–2009. *Biogeosciences* **10**, 4037–4054. (doi:10.5194/bg-10-4037-2013)
28. Sallée JB, Shuckburgh E, Bruneau N, Meijers AJS, Bracegirdle TJ, Wang Z. 2013 Assessment of Southern Ocean mixed-layer depths in CMIP5 models: historical bias and forcing response. *J. Geophys. Res. Oceans* **118**, 1845–1862. (doi:10.1002/jgrc.20157)
29. Galbraith ED, Gnanadesikan A, Dunne JP, Hiscock MR. 2010 Regional impacts of iron–light colimitation in a global biogeochemical model. *Biogeosciences* **7**, 1043–1064. (doi:10.5194/bg-7-1043-2010)
30. Geiderl RJ, MacIntyre HL, Kana TM. 1998 A dynamic regulatory model of phytoplanktonic acclimation to light, nutrients, and temperature. *Limnol. Oceanogr.* **43**, 679–694. (doi:10.4319/lo.1998.43.4.0679)
31. Li QP, Franks PJS, Landry MR, Goericke R, Taylor AG. 2010 Modeling phytoplankton growth rates and chlorophyll to carbon ratios in California coastal and pelagic ecosystems. *J. Geophys. Res. Biogeosci.* **115**, G04003. (doi:10.1029/2009JG001111)
32. Pfeil B *et al.* 2012 A uniform, quality controlled Surface Ocean CO₂ Atlas (SOCAT). *Earth Syst. Sci. Data Discuss.* **5**, 735–780. (doi:10.5194/essd-5-125-2013)
33. Sabine CL *et al.* 2012 Surface Ocean CO₂ Atlas (SOCAT) gridded data products. *Earth Syst. Sci. Data Discuss.* **5**, 781–804. (doi:10.5194/essdd-5-781-2012)
34. Takahashi T, Sutherland SC, Kozyr A. 2009 Global ocean surface water partial pressure of CO₂ database: measurements performed during 1968–2008 (version 2008). ORNL/CDIAC-152, NDP-088r.
35. Lovenduski NS, Gruber N, Doney SC, Lima ID. 2007 Enhanced CO₂ outgassing in the Southern Ocean from a positive phase of the southern annular mode. *Glob. Biogeochem. Cycles* **21**, GB2026. (doi:10.1029/2006GB002900)
36. Lenton A, Matear RJ. 2007 Role of the southern annular mode (SAM) in Southern Ocean CO₂ uptake. *Glob. Biogeochem. Cycles* **21**, GB2016. (doi:10.1029/2006GB002714)
37. Le Quéré C *et al.* 2007 Saturation of the Southern Ocean CO₂ sink due to recent climate change. *Science* **316**, 1735–1738. (doi:10.1126/science.1136188)
38. Metzl N. 2009 Decadal increase of oceanic carbon dioxide in southern Indian Ocean surface waters (1991–2007). *Deep Sea Res. II: Top. Stud. Oceanogr.* **56**, 607–619. (doi:10.1016/j.dsr2.2008.12.007)
39. Waugh DW, Primeau F, DeVries T, Holzer M. 2013 Recent changes in the ventilation of the southern oceans. *Science* **339**, 568–570. (doi:10.1126/science.1225411)
40. Lovenduski NS, Gruber N, Doney SC. 2008 Toward a mechanistic understanding of the decadal trends in the Southern Ocean carbon sink. *Glob. Biogeochem. Cycles* **22**, GB3016. (doi:10.1029/2007GB003139)
41. Dufour CO, Sommer JL, Gehlen M, Orr JC, Molines JM, Simeon J, Barnier B. 2013 Eddy compensation and controls of the enhanced sea-to-air CO₂ flux during positive phases of the southern annular mode. *Glob. Biogeochem. Cycles* **27**, 950–961. (doi:10.1002/gbc.20090)
42. Hauck J, Völker C, Wang T, Hoppema M, Losch M, Wolf-Gladrow DA. 2013 Seasonally different carbon flux changes in the Southern Ocean in response to the southern annular mode. *Glob. Biogeochem. Cycles* **27**, 1236–1245. (doi:10.1002/2013GB004600)

43. Le Quéré C, Takahashi T, Buitenhuis ET, Rödenbeck C, Sutherland SC. 2010 Impact of climate change and variability on the global oceanic sink of CO₂. *Glob. Biogeochem. Cycles* **24**, GB4007. (doi:10.1029/2009GB003599)
44. Morrison AK, Hogg AMcC. 2012 On the relationship between Southern Ocean overturning and ACC transport. *J. Phys. Oceanogr.* **43**, 140–148. (doi:10.1175/JPO-D-12-057.1)
45. Lovenduski NS, Long MC, Gent PR, Lindsay K. 2013 Multi-decadal trends in the advection and mixing of natural carbon in the Southern Ocean. *Geophys. Res. Lett.* **40**, 139–142. (doi:10.1029/2012GL054483)
46. Durack PJ, Wijffels SE, Matear RJ. 2012 Ocean salinities reveal strong global water cycle intensification during 1950 to 2000. *Science* **336**, 455–458. (doi:10.1126/science.1212222)
47. Dunne JP *et al.* 2012 GFDL's ESM2 global coupled climate–carbon Earth system models. Part I: physical formulation and baseline simulation characteristics. *J. Clim.* **25**, 6646–6665. (doi:10.1175/JCLI-D-11-00560.1)
48. Kamenkovich I, Cheng W, Schmid C, Harrison DE. 2011 Effects of eddies on an ocean observing system with profiling floats: idealized simulations of the Argo array. *J. Geophys. Res. Oceans* **116**, C06003. (doi:10.1029/2010JC006910)
49. Lee K *et al.* 2006 Global relationships of total alkalinity with salinity and temperature in surface waters of the world's oceans. *Geophys. Res. Lett.* **33**, L19605. (doi:10.1029/2006GL027207)
50. Johnson KS *et al.* 2009 Observing biogeochemical cycles at global scales with profiling floats and gliders: prospects for a global array. *Oceanography* **22**, 216–225. (doi:10.5670/oceanog.2009.81)
51. Cullison Gray SE, DeGrandpre MD, Moore TS, Martz TR, Friederich GE, Johnson KS. 2011 Applications of *in situ* pH measurements for inorganic carbon calculations. *Mar. Chem.* **125**, 82–90. (doi:10.1016/j.marchem.2011.02.005)
52. Weatherhead EC *et al.* 1998 Factors affecting the detection of trends: statistical considerations and applications to environmental data. *J. Geophys. Res. Atmos.* **103**, 17 149–17 161. (doi:10.1029/98JD00995)
53. Wanninkhof R *et al.* 2013 Global ocean carbon uptake: magnitude, variability and trends. *Biogeosciences* **10**, 1983–2000. (doi:10.5194/bg-10-1983-2013)
54. Vecchi GA, Harrison MJ. 2007 An observing system simulation experiment for the Indian Ocean. *J. Clim.* **20**, 3300–3319. (doi:10.1175/JCLI4147.1)
55. Meredith MP, Schofield O, Newman L, Urban E, Sparrow M. 2013 The vision for a Southern Ocean observing system. *Curr. Opin. Environ. Sustain.* **5**, 306–313. (doi:10.1016/j.cosust.2013.03.002)
56. Rintoul SR, Meredith MP, Schofield O, Newman L. 2012 The Southern Ocean observing system. *Oceanography* **25**, 68–69. (doi:10.5670/oceanog.2012.76)